

FAST PYROLYSIS OF AN ENSEMBLE OF BIOMASS PARTICLES IN A FLUIDIZED BED

O. S. Rabinovich, V. A. Borodulya,
L. M. Vinogradov, and V. V. Korban

UDC 620.0+66:658.567

A combined approach to the modeling of fast pyrolysis of biomass particles in a fluidized bed has been used. We used models of different levels: two models of pyrolysis of a single particle — with lumped and distributed parameters — and a model of pyrolysis of an ensemble of biomass particles based on the continuum equations for the gas blown through the bed and the equations of motion for individual particles. We have determined optimal (in terms of the biofuel yield) temperatures of the process for various particle sizes of wood biomass and various values of its moisture.

Keywords: fast pyrolysis, biomass, biofuel, pyrolysis kinetics, fluidized bed, computational hydrodynamics.

Introduction. Against the background of persistent economic problems connected with fossil fuels and the goal of the majority of states for diversification of the fuel-energy balance in the last few years, there has been a rising interest in obtaining liquid and gaseous fuels from biomass wastes resulting from the activities of the forest and wood-working industries, as well as from the agricultural sector. Production of liquid fuel, also called bio-oil, from biomass by thermochemical treatment is a promising trend of using reproducible types of energy. Bio-oil has certain advantages compared to gaseous products of biomass processing, among which is, in the first place, the possibility of easier and economic transportation from the place of production to the consumer.

The chief method for processing biomass into liquid fuel is fast pyrolysis [1, 2]. Providing a high yield of the liquid product requires a short time of heating a biomass particle in the reactor (of the order of a few seconds) and, what is particularly important, a short residence time of gaseous and condensable pyrolysis products in the high-temperature reactor zone needed to prevent their destruction. The above conditions can be realized in fluidized-bed reactors of various types [3–5] providing a high output and a high economic efficiency of the process. At the same time, the choice of optimal operating and design parameters of the reactor with a fluidized bed is a complex problem because of the strong temperature dependence of the pyrolysis rate of different components of the system and the close relation between the heating time of the particle and its size. Moreover, the particle size determines the maximum permissible blasting rate of the reactor influencing the most important parameter of the process — the residence time of gaseous condensable pyrolysis products in the reactor. In view of the foregoing, numerical modeling of the fast pyrolysis of biomass in a fluidized-bed reactor seems to be an effective method for optimizing the process.

The investigation of the biomass pyrolysis and gasification in a fluidized bed by the methods of numerical modeling has a long history, and the first works on these lines appeared as far back as the end of the 1980s (see the historical review in [6]). In these investigations, various levels of describing the pyrolysis process were used: from one-dimensional fluidized bed models with the simplest effective kinetics of thermal decomposition of biomass to multidimensional computational hydrodynamics models (CFD models) taking into account the individual pyrolysis kinetics of various components of the biomass and the transformations of the products formed. Among the recent works, noteworthy is the series of investigations carried out by K. Papadikis et al. [7–9], in which with the aid of CFD modeling the influence on the process of various factors is analyzed: heat and mass transfer between the biomass particles and the bed, sizes of particles and their shrinkage in the process of bio-oil output, etc.

However, despite the abundance of works on modeling the fast pyrolysis, many practically important points are still not clearly understood. Different approaches and methods of modeling have their own limitations and disad-

A. V. Luikov Heat and Mass Transfer Institute, National Academy of Sciences of Belarus, 15 P. Brovka Str., Minsk, 220072, Belarus. Translated from *Inzhenerno-Fizicheskii Zhurnal*, Vol. 83, No. 4, pp. 694–704, July–August, 2010. Original article submitted February 12, 2010.

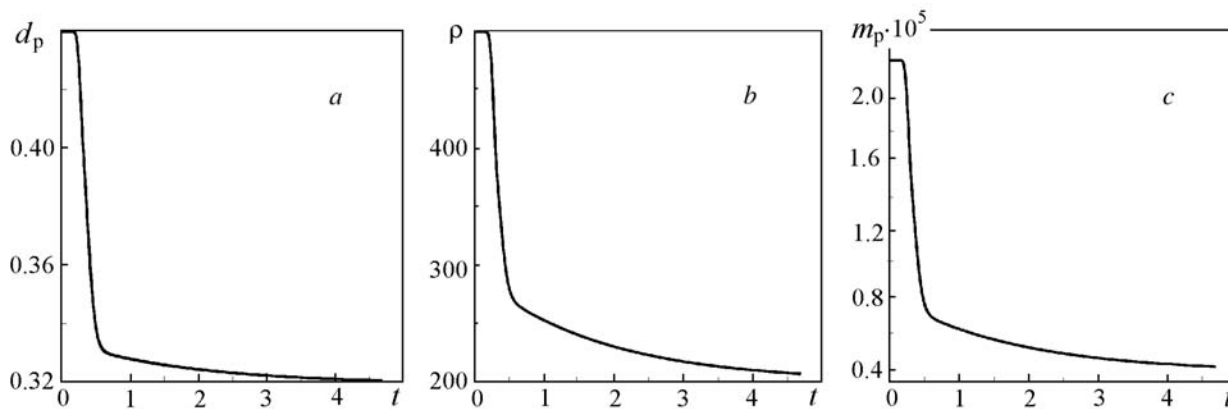


Fig. 1. Change with time in the biomass particle parameters for the optimal conditions found with the use of the one-dimensional phenomenological model: a) particle diameter; b) density; c) mass. d_p , mm; ρ , kg/m³; m_p , g; t , s.

vantages. In particular, one-dimensional and two-phase models of the fluidized bed do not give sufficient information on its spatial structure and on the motion of individual biomass particles, and the computing capacity of the CFD models is small and, therefore, cannot be used to describe the detailed pyrolysis kinetics of individual chemical components of the biomass.

In view of the foregoing, it should be recognized that the most plausible and effective way of studying the fast pyrolysis in a fluidized bed is a combination of several simulation techniques enabling one to consider the process at various levels complementing one another. In the present work, to investigate and optimize the fast pyrolysis of the biomass in a fluidized-bed reactor, we propose a combined approach consisting of sequential use of different numerical modules: 1) a model of pyrolysis of a single biomass particle with lumped parameters taking into account the detailed pyrolysis kinetics of various biomass components [10]; 2) a CFD model of an ensemble of biomass particles with effective pyrolysis kinetics; 3) a model of pyrolysis of a single particle with distributed parameters and detailed kinetics.

The above models were used in accordance with the following scheme:

1. Model 1 was used to determine the conditions for conducting the process that are optimal for the liquid biofuel yield and the time dependences of the particle density, diameter, and mass for the obtained optimal conditions.

2. With the use of the above dependences, as a result of the CFD modeling (model 2), the change with time in the average height of biomass particles in the reactor was determined; then the time dependence of the average height of biomass particles was converted to a dependence on the degree of completion of the process, η_p .

3. Assuming that the dependence of the average height of biomass particles on η_p has a universal character in a certain vicinity of parameters corresponding to the optimal conditions of the process, with the use of this dependence we made calculations by model 3 (model of a particle with distributed parameters and detailed kinetics) that enabled us to investigate more thoroughly the influence on the degree of conversion of the biomass to a liquid biofuel of such parameters as the temperature, the size of particles, and their moisture.

1. Input Data for the CFD Modeling of the Fast Pyrolysis of an Ensemble of Biomass Particles Obtained by the Model of a Single Particle with Lumped Parameters. Since the CFD modeling of the biomass pyrolysis with account for the detailed decomposition kinetics of individual components of wood requires too much computing time (with the existing capacity of the computers used), we used in the present work the pyrolysis dynamics of a single biomass particle (i.e., the time dependence of its density, diameter, and mass) calculated by the model with lumped parameters whose detailed description is given in [10]. From the viewpoint of this model the biomass particle is characterized by a set of averaged characteristics (temperature, density, and concentration of solid components) and the individual decomposition kinetics of wood components proposed in [11] is used. It was assumed that in the initial state the biomass has the following model chemical composition: 40% of cellulose, 35% of hemicellulose, and 25% of lignin.

For the base set of parameters, we took the following pyrolysis characteristics for the optimum variant found in [10]: biomass particle diameter $d_p = 0.44$ mm, diameter of inert particles of the fluidized bed $d_{in} = 0.94$ mm, and

reactor temperature $T_r = 773$ K. The changes in the diameter, density, and mass of the wood particle for this case calculated by the model of [10] are given in Fig. 1.

The dependences depicted in Fig. 1 are characterized by a small initial portion of duration about 0.2 s preceding the onset of pyrolysis in which heating and drying of the biomass particles takes place. Next a rapid change in the considered characteristics of the biomass particle occurs due to the cellulose and hemicellulose pyrolysis in the particle. Pyrolysis of these components of wood for the chosen conditions is completed in a time less than 1 s, and then the rate of change in the particle parameters slows down since the pyrolysis of the remaining lignin proceeds much slower.

The time dependences of the biomass particle parameters presented in Fig. 1 were used for further calculations of the behavior of an ensemble of such particles in the fluidized-bed reactor.

2. CFD Modeling of the Behavior of an Ensemble of Biomass Particles in the Fluidized Bed Reactor. To calculate the behavior of biomass particles in the reactor, we used the discrete element method [12] realized in the recent versions of the MFIX program package [13]. In this method, the motion of solid particles is described by the Newton equation of motion, whereas the gas flow is considered from the viewpoint of continuum motion theory (Navier–Stokes equations). Modeling was carried out in a two-dimensional formulation (pseudothree-dimensional case) in which the calculation domain represented a flat layer with a thickness of one calculation cell equal to the diameter of maximum-size particles. The interparticle interaction is given in the method under consideration by the soft sphere model of [14]. The momentum exchange between the gaseous phase and discrete particles is calculated by means of local averaging of the parameters of the gaseous and solid phases over the calculation cell volume [15]. In calculating the interaction forces of the gas and particles, an important parameter is the portion of the calculation cell volume ε_g occupied by the gas. In the present work, we used a modified, more exact method for calculating the value of this quantity taking into account that the solid phase particle can be at the boundary of the calculation cell and part of its volume extends into adjacent cells. Let us consider this in more detail.

In the three-dimensional case (3D), the calculation of the ε_g value is based on the calculation of the volumes of particles entering into the cells, i.e.,

$$\varepsilon_g^{3D} = 1 - \frac{\sum_i V_{p,i}}{V_{\text{cell}}} . \quad (1)$$

The analogous value in the case of pseudothree-dimensional modeling (2D) is calculated in terms of the cross-section area of the particles residing in the cell:

$$\varepsilon_g^{2D} = 1 - \frac{\sum_i S_{p,i}}{S_{\text{cell}}} . \quad (2)$$

To pass to the three-dimensional volume fraction of the gas used in calculating the particle-gas interaction force, the transformation proposed in [16] is used:

$$\varepsilon_g^{3D} = 1 - \frac{2}{\sqrt{\pi\sqrt{3}}} (1 - \varepsilon_g^{2D})^{3/2} . \quad (3)$$

In formulas (1) and (2), summation is made over all particles whose centers lie inside the cell under consideration. In the present work, we propose a modification of formula (2): in the case where not the whole of the particle is in the cell being analyzed, instead of the total cross-section area of the particle S_p , only that part of this area S'_p enters into formula (2) that lies in the cell under consideration. In calculating S'_p , different variants of the particle position in the cell are analyzed: the whole of the particle is inside the cell, it crosses one of its boundaries, and it crosses two boundaries of the cell (is near the cell corner).

The increase in the accuracy of calculating ε_g obtained as a result of using the proposed technique has made it possible to achieve a good agreement of the minimal fluidization rates calculated in the CFD model with the known

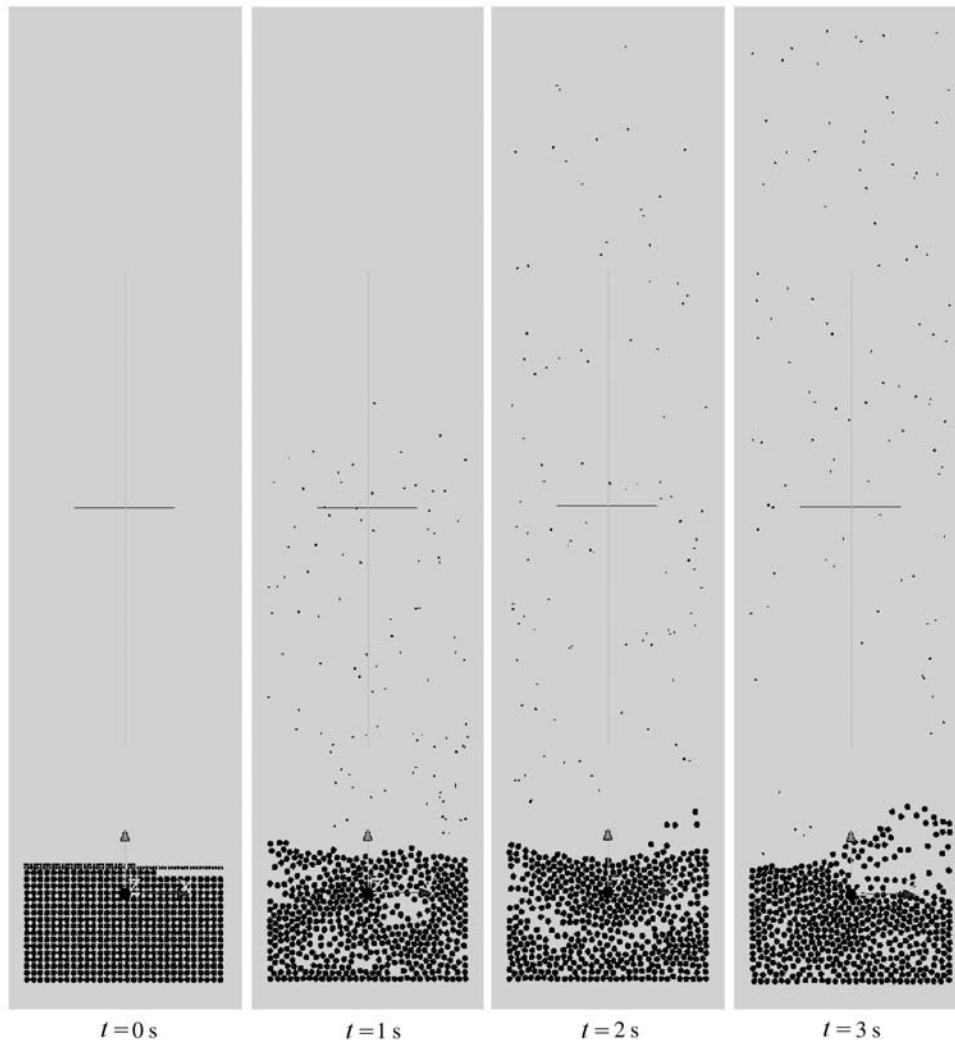


Fig. 2. Change with time in the configuration of an ensemble of biomass particles in the course of their pyrolysis in a reactor with a fluidized bed of sand; biomass particles are represented by blue dots, bed particles — by brown circles.

experimental correlations [17]. Such agreement is one of the main criteria for the adequacy of calculations carried out with the use of methods of computational hydrodynamics.

The behavior of an ensemble of biomass particles in their fast pyrolysis in a fluidized-bed reactor was investigated by means of three-dimensional modeling in the MFIX package. The reactor temperature and the parameters of biomass particles and inert particles of the bed were chosen on the basis of the process optimization for the liquid fuel yield carried out with the help of the particle pyrolysis model with lumped parameters and detailed decomposition kinetics of the wood components (see item 1). The modeled reactor represented a rectangular space of width 3 cm and height 14 cm. Since calculations were performed for the pseudo-three-dimensional case, the reactor thickness was taken equal to the diameter of the largest particles, 0.94 mm. In the model, the motion of 500 inert particles (quartz sand) and 100 biomass particles was considered. The calculation domain was split into square cells with a side of 0.17 cm. In the calculations, the following characteristics of the CFD model were used:

Reactor temperature	775
	<i>Gas phase (nitrogen)</i>
Density	0.43 kg/m ³
Viscosity	3.76·10 ⁻⁵ Pa·s
Fluidizing gas velocity	0.53 m/s

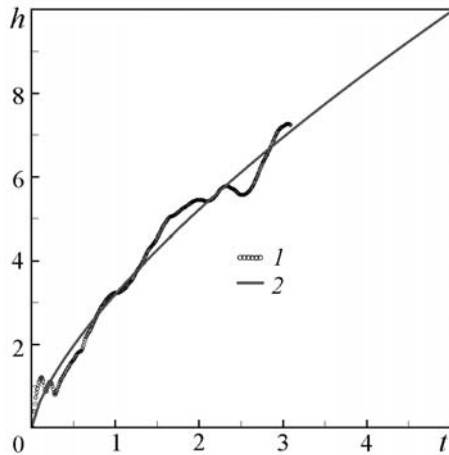


Fig. 3. Change with time in the mean height of the ensemble of biomass particles above the bed: 1) results of the CFD modeling; 2) approximation of the equation $h = ax^b$, where $a = 3.20044$, $b = 0.70456$. h , cm; t , s.

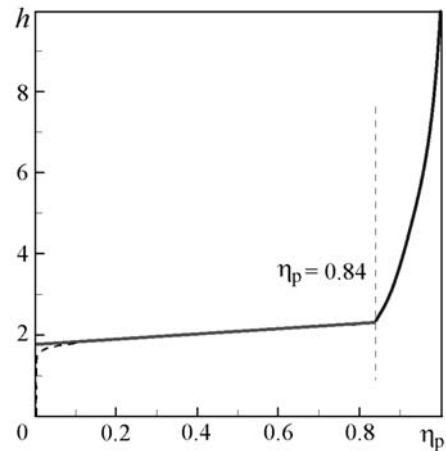


Fig. 4. Change in the mean height of biomass particles above the fluidized bed as a function of the parameter η_p ; dashed line — calculated curve; solid line — approximation; two characteristic portions of the dependence $h(\eta_p)$ are clearly seen.

Particles

Initial density of biomass particles	500 kg/m ³
Bed particle number density	2640 kg/m ³
Initial diameter of biomass particles	0.44 mm
Diameter of bed particles	0.94 mm
Friction coefficient	0.1
Coefficient of damping	$0.85 \cdot 10^{-3}$ N·s/m
Coefficient of rigidity	10^2 N/m

At the initial instant of time all biomass particles had an equal size. The change with time in the configuration of the ensemble of biomass particles in the course of pyrolysis is shown in Fig. 2. As is seen, with decreasing mass of the wood particles they are ejected higher and higher above the bed surface as a result of random collisions with heavier and larger particles of the fluidized bed, as well as due to the action of the gas jets.

The change with time in the average height of biomass particles above the bed surface is given in Fig. 3. This dependence calculated by means of CFD modeling is well approximated by the power function. The obtained correlation was found for the given particular set of pyrolysis process characteristics and, naturally, its parameters will vary widely with a change in these characteristics. In the present work, we propose that the dependence of the mean height of an ensemble of biomass particles on the parameter characterizing the degree of completion of the pyrolysis process is more universal. The quantity $\eta_p = \frac{m_{v0} - m_{p,d}}{m_{v0} - m_{p,f}}$ was used as such a dependence. To determine the finite mass

of the particle $m_{p,f}$, we assumed that the density of the coke formed by pyrolysis was 150–200 kg/m³, and the mass fraction of the obtained coke with respect to the initial mass of the particle constituted 15–20%. It was also assumed that in the process of pyrolysis the particle shrinks and its diameter measures about 0.8 of the initial one.

As a result of passing to the parameter η_p as a factor determining the position of the biomass particle in the reactor, the dependence of the mean height of particles on this parameter shown in Fig. 4 was obtained. A characteristic feature of the function $h(\eta_p)$ is the fact that the biomass particle subjected to pyrolysis in the major portion of the interval of degrees of conversion is near the fluidized bed surface, and only at $\eta_p > 0.84$ does it begin to be carried by the gas flow out of the reactor. The dependence of the biomass particle height on the degree of completion of

the pyrolysis process was approximated with account for the above feature on segments $[0, 0.84]$ and $[0.84, 1]$ by the following linear and polynomial functions:

$$h = 1.7731 + 0.6466\eta_p, \quad 0 < \eta_p < 0.84;$$

$$h = -151777 + 847031\eta_p - 1889430\eta_p^2 + 2105820\eta_p^3 - 1172704\eta_p^4 + 261070\eta_p^5, \quad 0.84 < \eta_p < 1. \quad (4)$$

Approximation (4) was considered as approximately valid in some vicinity of the optimal set of parameters of the pyrolysis process and was used further in the calculations and optimization with the aid of the one-dimensional model of pyrolysis of a single biomass particle with distributed parameters.

3. Investigation of the Fast Pyrolysis of a Single Biomass Particle by Means of the Model with Distributed Parameters. The range of applicability of the biomass particle pyrolysis model with lumped parameters used in [10] and in item 1 of the present paper is limited to the particle size up to 1 mm. At larger diameters of biomass particles the distributions of the temperature and concentrations of biomass components in the particle remain nonuniform practically throughout the pyrolysis time and, as a result of the strong temperature nonlinearity of the process, they cannot be described by averaged values. More detailed information on the distribution of pyrolysis characteristics over the particle during the entire process can be obtained by means of detailed (local) description of the heat and mass transfer in the particle in which in the one-dimensional approach the process characteristics are distributed over the particle radius.

Phases, components, and their characteristics. According to the proposed model, at each point inside the biomass particle being processed in the general case, components of three phases, solid, liquid, and gaseous ones, can be present. Let us denote the volume-mean densities of these phases as ρ_s , ρ_{liq} , and ρ_g . In the detailed kinetic model of biomass pyrolysis [11] used in the present work, the following components of the solid phase participate: the initial components of the wood — cellulose, hemicellulose, and lignin (respectively, with densities ρ_{v1} , ρ_{v2} , ρ_{v3}) and activated modifications of these components (densities ρ_{a1} , ρ_{a2} , and ρ_{a3} , respectively) formed by their depolymerization under the action of the temperature. Moreover, a component of the solid phase is pyrolytic coke with density ρ_c .

The portions of the space occupied by each of the basic condensed components (biomass, coke, and moisture) can be defined as the ratio of the volume-mean density to the "true" density of a given component designated by the superscript $\hat{\cdot}$:

$$\varepsilon_s = \frac{\rho_s}{\hat{\rho}_s}; \quad \varepsilon_c = \frac{\rho_c}{\hat{\rho}_c}; \quad \varepsilon_{liq} = \frac{\rho_{liq}}{\hat{\rho}_{liq}}. \quad (5)$$

In view of this definition,

$$\varepsilon_s + \varepsilon_{liq} + \varepsilon_g = 1. \quad (6)$$

For simplicity, we assume that the three initial chemical components of the wood have an equal "true" density.

Denote by the index 0 the density values (as well as the values of other parameters) in the source material. In particular, ρ_{v0} is the density of the source dry wood.

According to the adopted kinetic pyrolysis model, the gas phase with density ρ_g has the following composition: water vapor (mass fraction ξ_{liq}), high-molecular gas components capable of condensing upon cooling and forming a liquid biofuel — bio-oil (total mass fraction ξ_l), and light fractions noncondensable under standard conditions (total mass fraction ξ_g), and an inert fluidizing component (ξ_{in}).

In the first stage of processing the biofuel particle, the latter gives off the moisture contained in it. For large particles (with a diameter of a few millimeters), the drying and pyrolysis stage may overlap. The velocity of motion of the drying zone is determined, as a rule, by the heat supply velocity for the moisture to evaporate and not by the evaporation kinetics. Therefore, the traditional drying models consider the evaporation front displacement calculated as

a result of solving the Stefan problem. In the present work, however, we use the general approach based on the through calculation (from the center of the particle to its outer boundary) of continuous distributions of all physical parameters of the system, including the moisture concentration in the particle. The application of a sufficiently fine spatial mesh permits isolating a narrow evaporation region with a large moisture concentration gradient.

To calculate the motion of the evaporation zone, the first-order effective kinetics for the moisture concentration is introduced:

$$\frac{d\rho_{\text{liq}}}{dt} = -k_{\text{ev}}\rho_{\text{liq}}. \quad (7)$$

The following expression for the evaporation rate was used in the present work:

$$k_{\text{ev}} = \begin{cases} 1 \cdot 10^6 \exp(-4817/T) \text{ (s}^{-1}\text{)}, & T \geq 380 \text{ K and } \rho_{\text{liq}} > 0; \\ 1 \cdot 10^6 \exp(-4817/T) \exp[-2(380 - T)] \text{ (s}^{-1}\text{)}, & T < 380 \text{ K or } \rho_{\text{liq}} = 0. \end{cases} \quad (8)$$

Transfer of energy and gaseous components inside the particle. The temperature inside the model spherical particle being processed is determined from the energy equation

$$\begin{aligned} (\rho_v c_{pv} + \rho_c c_{pc} + \rho_{\text{liq}} c_{p\text{liq}}) \frac{\partial T}{\partial t} &= \frac{1}{r^2} \frac{\partial}{\partial r} \left(r^2 \lambda_{\text{eff}} \frac{\partial T}{\partial r} \right) - G c_{pg} \frac{1}{r^2} \frac{\partial (r^2 T)}{\partial r} \\ &- Q_{\text{ev}} \Phi_{\text{liq}} + \sum_{n=1}^3 \sum_{m=1}^3 Q_{nm} \Phi_{nm} + Q_4 \rho_g k_4 \xi_t. \end{aligned} \quad (9)$$

At the outer boundary of the particle, the conditions for the heat exchange with the working medium of the reactor described in detail in [10] are specified.

For the gas phase, the approximation of the quasi-stationary mass flow, meaning the absence of reactants accumulation in the pore space of the biomass particles, holds:

$$\frac{1}{r^2} \frac{\partial (r^2 G)}{\partial r} = \Phi_{\text{liq}} + \Phi_g + \Phi_t. \quad (10)$$

Mass transfer of the gas components ξ_j occurs due to the convection (the index j is common for the following gas components: t — condensable components (tars), g — noncondensable components, liq — water vapor):

$$\frac{\partial (\varepsilon_g \rho_g \xi_j)}{\partial t} + \frac{1}{r^n} \frac{\partial (r^n G \xi_j)}{\partial r} = \Phi_j, \quad (11)$$

where Φ_j is the mass rate of formation of the j th component. Remaining within the framework of the quasi-stationary approximation, for the mass flows of gaseous components from Eq. (11) we get

$$\frac{1}{r^2} \frac{\partial (r^2 G_j)}{\partial r} = \Phi_j, \quad (12)$$

where $G_j = G \xi_j$.

The boundary conditions for convective and radiative heat exchange of the biomass particle with its environment in the reactor were formulated in much the same manner as in [10]. The equations of mass transfer in the particle in the adopted formulation do not require specifying the boundary conditions at its outer boundary. The thermal and mechanical properties of the system's components also coincide with those used in [10].

Shrinkage of the biomass particle in the process of pyrolysis. We used the elementary model of particle shrinkage based on comparing the current mass of the coke formed from the particle with a certain mean standard value of the final residual coke mass. In so doing, the final coke density $\rho_{c,f}$ is assumed to be independent of the chemical component of the wood from which it was formed. The standard mean final mass fraction of the coke obtained from the wood biomass is equal to the ratio of the standard final mass of the coke $m_{c,f}$ formed by pyrolysis to the initial mass of dry wood m_{v0} : $\chi_{st} = \frac{m_{c,f}}{m_{v0}}$. From the mass balance condition it follows that $\chi_{st}\rho_{v0}V_0 = \rho_{c,f}V_f$. Then

$$\text{the relative standard volume shrinkage } \sigma_{st} = \frac{V_0 - V_f}{V_0} = 1 - \chi_{st} \frac{\rho_{v0}}{\rho_{c,f}}.$$

Let at some instant of time at an arbitrary point of the particle (in a small vicinity of volume dV) some current fraction of the coke formed $\mu_c = \frac{\rho_c}{\rho_{v0}}$ be present. To calculate the local shrinkage of the particle at this point, let us use the hypothesis that this shrinkage depends linearly on the ratio $\rho_c/\rho_{c,f}$:

$$\sigma = \frac{dV_0 - dV}{dV_0} = \sigma_{st} \frac{\rho_c}{\rho_{c,f}} = \sigma_{st} \mu_c \frac{\rho_{v0}}{\rho_{c,f}} = \left(1 - \chi_{st} \frac{\rho_{v0}}{\rho_{c,f}}\right) \mu_c \frac{\rho_{v0}}{\rho_{c,f}}. \quad (13)$$

If we introduce the density ratio between the source wood and the coke $\zeta = \rho_{v0}/\rho_{c,f}$, then the local shrinkage will be written in a more compact form:

$$\sigma = (1 - \chi_{st}\zeta) \zeta \mu_c. \quad (14)$$

Proceeding from the definition of the local shrinkage, we can construct a numerical procedure for calculating the particle deformations at each time integration step of the system of equations describing the pyrolysis.

Consider a particle at some instant of time $t^{(n)}$. As a result of the numerical discretization, at this instant of time the particle is split into concentric spherical layers with radii $r_i^{(n)}$ (layer numbers increase from the center, $i = 1, \dots, N$). The current splitting of the particle into spherical layers is a result of its evolution from the initial state in which it was split into layers of equal thickness with corresponding radii $r_{i,0} = i\Delta r_0$ (Δr_0 is the initial step of splitting). The position of the layer boundaries at the next time step $t^{(n+1)}$ is calculated upon determining the coke concentration in each layer at this step. This calculation begins from the first (internal) layer of the particle. From the expression for the local shrinkage (14) it follows that

$$\frac{[r_{2,0}^3 - (r_2^{(n+1)})^3]}{r_{2,0}^3} = \sigma_{3/2}^{(n+1)} = (1 - \chi_{st}\zeta) \zeta \mu_{3/2}^{(n+1)}. \quad (15)$$

Hence we find $r_2^{(n+1)}$:

$$r_2^{(n+1)} = r_{2,0} (1 - \sigma_{3/2}^{(n+1)})^{1/3}. \quad (16)$$

Then the layer radii $r_i^{(n+1)}$, $i = 3, \dots, N$, are calculated recursively. For instance, if the radius $r_{i-1}^{(n+1)}$ is known, then the radius $r_i^{(n+1)}$ can be found from the relation

$$\frac{r_{i,0}^3 - r_{i-1,0}^3 - [(r_i^{(n+1)})^3 - (r_{i-1}^{(n+1)})^3]}{r_{i,0}^3 - r_{i-1,0}^3} = \sigma_{i-1/2}^{(n+1)} = (1 - \chi_{st}\zeta) \zeta \mu_{i-1/2}^{(n+1)}. \quad (17)$$

Then

$$r_i^{(n+1)} = [(r_{i-1}^{(n+1)})^3 + (r_{i,0}^3 - r_{i-1,0}^3) (1 - \sigma_{i-1/2}^{(n+1)})]^{1/3}. \quad (18)$$

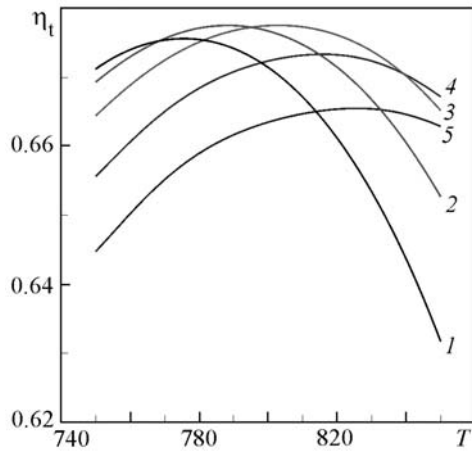


Fig. 5. Dependence of the liquid biofuel yield on the reactor temperature at various diameters of biomass particles ($\phi = 8\%$): 1) $d_p = 0.5$ mm; 2) 0.7; 3) 1.0; 4) 1.4; 5) 2.0. T , K.

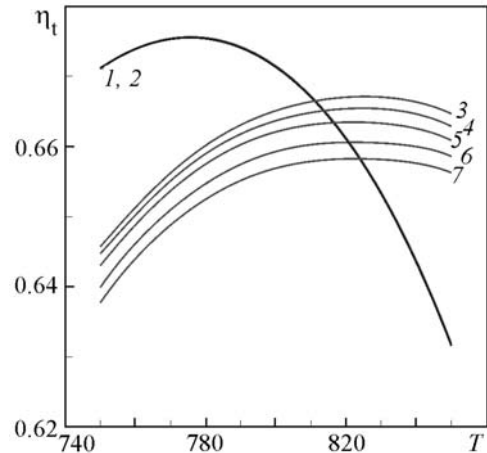


Fig. 6. Dependence of the liquid biofuel yield on the reactor temperature at various values of the source biomass moisture: 1) $d_p = 0.5$ mm, $\phi = 0\%$; 2) 0.5, 40; 3) 2.0, 0; 4) 2.0, 8; 5) 2.0, 16; 6) 2.0, 32; 7) 2.0, 40. T , K.

Decomposition of volatile pyrolysis products. The heavy fractions released by the particle pyrolysis and forming the basis for the condensable liquid product decompose partly when moving together with the gas flow in the reactor. The amount of obtained heavy fractions is determined by the process temperature and their residence time in the reactor, so that the degree of conversion of the biomass into a liquid biofuel can be calculated as follows:

$$\eta_t = \frac{\int_0^{t_{\text{pir}}} 4\pi r_p^2 (G\xi_t)_e \exp[-k_4(T_r) t_r(t)] dt}{m_{v0}}, \quad (19)$$

where $(G\xi_t)_e$ is the density of the mass flow of gaseous heavy fractions from the particle surface; $k_4(T_r)$ is the decomposition constant of volatile pyrolysis products; $t_r(t)$ is the residence time in the reactor of the portion of volatiles released at time t ; m_{v0} is the initial mass of the wood particle.

Using the approximation of the dependence of the mean height of the particle on the degree of completion of pyrolysis $h(\eta_p)$ (4) obtained by means of CFD modeling, we calculate the residence time of volatile pyrolysis products in the reactor as $t_r = h(\eta_p)/U_g$.

Analysis of the results of using the distributed-parameter model. The above-described model of biomass particle pyrolysis taking into account the distribution of the temperature and concentrations of the chemical components inside the particle as well as using the data on the change in the mean height of particles in the reactor in the process, obtained by means of CFD modeling, has made it possible to redefine the parameters of optimal regimes of fast pyrolysis. In the first place, refinements concern large-size biomass particles, since for such particles the model with particle-averaged characteristics turns out to be too crude. The calculations made have shown that as the biomass particle diameter increases from 0.44 to 2.0 mm, the degree of biomass conversion into a liquid fuel decreases insignificantly — from 68 to 66%, and the optimal temperature of the process has to be increased thereby from 775 to 820 K (Fig. 5).

The model with distributed parameters has also made it possible to investigate the influence of the initial moisture of biomass particles on the end product yield (Fig. 6). For small-size particles, moisture practically does not influence the liquid biofuel yield: the temperature dependences of the degree of conversion into bio-oil $\eta_t(T)$ for particles of diameter 0.5 mm at the initial moisture of particles 0 and 40% coincide (curves 1 and 2 in Fig. 6). This is due to the fact that for small particles their heating and drying time is short compared to the period of their complete pyrolysis, drying of the particle is completed at an early stage of the process, and the pyrolysis stage is then largely

independent. With increasing sizes of biomass particles the restrictions on the heat transport into the heating and drying zone begin to play an increasingly important role. In this case, the drying and pyrolysis stages begin to overlap in time, and the residence time of condensable pyrolysis products in the particle and in the reactor increases. As a result, for large particles the degree of conversion into bio-oil decreases as their initial moisture increases (curves 3–7 for particles of diameter 2 mm in Fig. 6).

Conclusions. The numerical investigations of the fast pyrolysis of biomass in a fluidized-bed reactor based on the CFD modeling by the discrete element method have made it possible to redefine the optimal conditions for conducting the process. From the results of numerical modeling, the dependence of the mean position (on the vertical coordinate) of biomass particles on the time and on the degree of completion of the pyrolysis process has been determined. This dependence has been used to investigate the process with the aid of a simpler one-dimensional model taking into account the detailed pyrolysis kinetics of various components of wood and the distribution of the temperature and concentrations of solid, liquid, and gaseous components in it. The influence of the particle size and initial moisture of the biomass on the liquid biofuel yield in the process of fast pyrolysis has been investigated. It has been shown that an increase in the size of the original biomass particles leads to a decrease in the degree of biomass — bio-oil conversion; however, this negative effect can be compensated to a large extent by controlling the temperature of the reactor and the velocity of its blow. At the same time, to hold constant the high parameters of the process with increasing sizes of the original biomass particles, it is necessary to place more stringent requirements upon its initial moisture, since for large particles the negative influence of the drying stage on the process of fast pyrolysis becomes more significant.

NOTATION

c_p , heat capacity, J/(kg·K); d_p , diameter of the biomass particle, m; d_{in} , diameter of the inert bed (sand) particle, m; G , specific mass flow of the gas, kg/(m²·s); h , mean position of the biomass particle above the fluidized bed surface; k_4 , decomposition constant of volatile condensable pyrolysis products, s⁻¹; k_{ev} , moisture evaporation constant in the biomass particle, s⁻¹; m_p , current mass of the particle, kg; m_{v0} , initial dry mass of the wood particle, kg; Q , thermal effect of conversion, J/kg; r , distance to the center of the biomass particle, m; S_p , cross-section area of the particle, m²; T , local temperature in the biomass particle, K; t , time, s; t_{pir} , total time of biomass particle pyrolysis, s; U_g , blow velocity of the reactor, m/s; V_p , particle volume, m³; ξ , portion of the space occupied by a phase or a chemical component; η_t , degree of biomass conversion into a liquid biofuel; η_p , degree of completion of biomass particle pyrolysis; λ_{eff} , effective heat conductivity of the biomass particle, W/(m·K); ξ_j , relative mass concentration of the j th gas component; ρ , density, kg/m³; ρ_{v0} , source wood density, kg/m³; σ , relative volume shrinkage of the biomass particle; Φ , reaction (phase transition) rate, kg/(s·m³); $\chi_{st} = m_{c,f}/m_{v0}$, standard ratio of the mass of coke formed to the initial dry mass of the wood particle. Subscripts: a, activated biomass; c, coal; d, dry, e, outer boundary of the particle; eff, effective; ev, evaporation; f, final; g, gas; in, inert; liq, liquid; p, particle; pir, pyrolysis; r, reactor; s, solid; st, standard; t, tar (liquid biofuel); v, source biomass; 0, initial.

REFERENCES

1. D. A. Laird, R. C. Brown, J. E. Amonette, and J. Lehmann, Review of the pyrolysis platform for coproducing bio-oil and biochar, *Biofuels, Bioprod. Bioref.*, **3**, 547–562 (2009).
2. D. Mohan, Ch. U. Pittman Jr., and Ph. H. Steele, Pyrolysis of wood/biomass for bio-oil: A critical review, *Energy Fuels*, **20**, 848–889 (2006).
3. I. Ph. Boukis, P. Grammelis, S. Bezergianni, and A. V. Bridgwater, CFB air-blown flash pyrolysis. Part I: Engineering design and cold model performance, *Fuel*, **86**, 1372–1386 (2007).
4. I. Ph. Boukis, S. Bezergianni, P. Grammelis, and A. V. Bridgwater, CFB air-blown flash pyrolysis. Part II: Operation and experimental results, *Fuel*, **86**, 1387–1395 (2007).
5. J. Yanik, C. Kornmayer, M. Saglam, and M. Yuksel, Fast pyrolysis of agricultural wastes: Characterization of pyrolysis products, *Fuel Process. Technol.*, **88**, 942–947 (2007).

6. P. Basu and P. Kaushal, Modeling of pyrolysis and gasification in fluidized beds, *Chem. Prod. Process Model.*, **4**, Issue 1, Art. 21 (2009).
7. K. Papadikis, A. V. Bridgwater, and S. Gu, CFD modelling of the fast pyrolysis of biomass in fluidized bed reactors. Part A: Eulerian computation of momentum transport in bubbling fluidised beds, *Chem. Eng. Sci.*, **63**, Issue 16, 4218–4227 (2008).
8. K. Papadikis, S. Gu, and A. V. Bridgwater, CFD modelling of the fast pyrolysis of biomass in fluidized bed reactors. Part B: Heat, momentum, and mass transport in bubbling fluidized beds, *Chem. Eng. Sci.*, **64**, Issue 5, 1036–1045 (2009).
9. K. Papadikis, S. Gu, and A. V. Bridgwater, Computational modelling of the impact of particle size to the heat transfer coefficient between biomass particles and a fluidized bed, *Fuel Process. Technol.*, **91**, Issue 1, 68–79 (2010).
10. O. S. Rabinovich, V. V. Korban, G. I. Pal'chenok, and O. P. Khorol'skaya, Modeling of fast pyrolysis of a single biomass particle in an inert boiling bed, *Inzh.-Fiz. Zh.*, **82**, No. 4, 621–631 (2009).
11. R. S. Miller and J. Bellan, A generalized biomass pyrolysis model based on superimposed cellulose, hemicellulose and lignin kinetics, *Combust. Sci. Technol.*, **126**, 97–137 (1997).
12. Y. Tsuji, T. Kawaguchi, and T. Tanaka, Discrete particle simulation of two-dimensional fluidized bed, *Powder Technol.*, **77**, 79–87 (1993).
13. M. Syamlal, W. Rogers, and T. O'Brien, *MFIX Documentation Theory Guide*, U.S. Department of Energy (1993).
14. P. A. Cundall and O. D. Strack, A discrete numerical model for granular assemblies, *Geotechnique*, **291**, 47–65 (1979).
15. T. B. Anderson and R. Jackson, A fluid mechanical description of fluidized beds, *Industr. Eng. Chem. Fundam.*, **6**, 527–539 (1967).
16. B. P. B. Hoomans, J. A. M. Kuipers, W. J. Briels, and W. P. M. V. Swaaij, Discrete particle simulation of bubble and slug formation in a two-dimensional gas-fluidized bed: a hard sphere approach, *Chem. Eng. Sci.*, **51**, No. 1, 99–118 (1996).
17. D. Kunii and O. Levenshpiel, *Fluidization Engineering* [Russian translation], Khimiya, Moscow (1976).